Overexpression and altered nucleocytoplasmic distribution of *Anopheles* ovalbumin-like SRPN10 serpins in *Plasmodium*-infected midgut cells

Alberto Danielli,[1,2] Carolina Barillas-Mury,[3,4]
Sanjeev Kumar,[4] Fotis C. Kafatos[1]* and
Thanasis G. Loukeris[1,5]*

[1]*European Molecular Biology Laboratory (EMBL),
Meyerhoftrasse 1, 69117 Heidelberg, Germany.*
[2]*Dipartimento di Biologia Evoluzionistica Sperimentale,
Università di Bologna, Via Selmi 3, 40126 Bologna, Italy.*
[3]*Colorado State University, Department of Microbiology,
Immunology and Pathology (MIP), 1619 Campus Delivery,
Fort Collins, CO, USA.*
[4]*Laboratory of Malaria and Vector Research, National
Institutes of Health, 4 Center Drive, Bethesda, MD 20892,
USA.*
[5]*Institute of Molecular Biology and Biotechnology (IMBB/
FORTH), Vassilika Vouton, GR71110, Heraklion, Greece.*

Summary

The design of effective, vector-based malaria transmission blocking strategies relies on a thorough understanding of the molecular and cellular interactions that occur during the parasite sporogonic cycle in the mosquito. During *Plasmodium berghei* invasion, transcription from the SRPN10 locus, encoding four serine protease inhibitors of the ovalbumin family, is strongly induced in the mosquito midgut. Herein we demonstrate that intense induction as well as redistribution of SRPN10 occurs specifically in the parasite-invaded midgut epithelial cells. Quantitative analysis establishes that in response to epithelial invasion, SRPN10 translocates from the nucleus to the cytoplasm and this is followed by strong SRPN10 overexpression. The invaded cells exhibit signs of apoptosis, suggesting a link between this type of intracellular serpin and epithelial damage. The SRPN10 gene products constitute a novel, robust and cell-autonomous marker of midgut invasion by ookinetes. The SRPN10 dynamics at the subcellular level confirm and further

elaborate the 'time bomb' model of *P. berghei* invasion in both *Anopheles stephensi* and *Anopheles gambiae*. In contrast, this syndrome of responses is not elicited by mutant *P. berghei* ookinetes lacking the major ookinete surface proteins, P28 and P25. Molecular markers with defined expression patterns, in combination with mutant parasite strains, will facilitate dissection of the molecular mechanisms underlying vector competence and development of effective transmission blocking strategies.

Introduction

In arthropods, including insects, serpins have to date been identified principally as secreted haemolymph proteins (Kanost, 1999). Genetic and biochemical studies in *Drosophila* have identified extracellular serpins, together with their target proteases, as principal regulators of antimicrobial responses, the melanization cascade and establishment of the dorsoventral axis (Ligoxygakis *et al.*, 2002a; Ligoxygakis *et al.*, 2002b; Ligoxygakis *et al.*, 2003). Lately, genome sequencing projects have revealed a large number of annotated serpins in both the fruit fly (Adams *et al.*, 2000; Kruger *et al.*, 2002) and *Anopheles gambiae* (Christophides *et al.*, 2002; Holt *et al.*, 2002), many of which lack an obvious hydrophobic signal sequence and therefore are predicted to be intracellular. Functional characterization of these serpins and their targets is expected to uncover additional biological roles of this important class of molecules.

Recently, we have cloned the *A. gambiae* SRPN10 locus and determined that it encodes four alternatively spliced serpins with similarity to intracellular, nucleocytoplasmic serpins of the ovalbumin clade (Danielli *et al.*, 2003), some of which are involved in modulation of apoptotic processes in mammals (Bird, 1998; Silverman *et al.*, 2001). We have shown that at least three SPRN10 isoforms are functional inhibitors of different types of proteases *in vitro*, including bacterial subtilisins, and that the *SRPN10* gene is strongly upregulated in the midgut after infection by the model rodent parasite *Plasmodium berghei*. This finding is particularly interesting as the midgut appears to be an especially difficult barrier for the parasite in order to complete the sporogonic cycle in the

vector: even in susceptible mosquitoes major losses of parasite numbers occur during midgut invasion (Sinden, 1999). Moreover, genetically defined mechanisms of refractoriness (Collins *et al.*, 1986; Vernick *et al.*, 1995) operate during or immediately after midgut invasion. Detailed characterization of *Anopheles* genes with altered expression profile during midgut invasion is therefore important to understand the molecular mechanisms underlying vector competence.

The present study introduces the products of the *SRPN10* gene as robust cytological invasion marker. Its overexpression reflects local changes in the cell(s) invaded by the parasite, allowing a detailed description of the dynamics of ookinete invasion and associated phenomena at the cellular and subcellular level. Results using wild-type parasites are consistent with and further elaborate the 'time bomb' model of intracellular invasion, for both *A. gambiae* and *A. stephensi*. Significantly, use of the serpin marker with an invasion-deficient double-knockout *P. berghei* strain that lacks two major surface proteins, P28 and P25, has revealed interesting differences in the midgut invasion process, in both vector species.

Results

Midgut cells associated with invading ookinetes strongly overexpress SRPN10

On the basis of RNA blot analysis and reverse transcription polymerase chain reaction (RT-PCR) we reported that transcripts of the *SRPN10* gene are more abundant at the time when *P. berghei* ookinetes are crossing the midgut (Danielli *et al.*, 2003). Herein we have used a SRPN10-specific, affinity-purified antibody in confocal microscopy studies, to reveal the detailed, cellular and subcellular spatial distribution of SRPN10 in the mosquito midgut epithelium during its invasion by ookinetes. Pre-immune serum was used as a negative control (Fig. 1A).

The non-infected control midguts of bloodfed *A. gambiae* show rather diffuse, low intensity staining for SRPN10. Higher magnification reveals protein localization primarily in the nucleus, with minor amounts in the cytoplasm (Fig. 1B, insets). Only a few, sporadic cells exhibit stronger cytoplasmic SRPN10 levels in non-infected midguts (Fig. 1B). By contrast, in the *Plasmodium*-infected midgut, numerous cells are stained intensely, revealing a strong and spatially regulated overexpression of SRPN10 (Fig. 1C). Remarkably, SRPN10 overexpressing cells are closely and almost invariably associated with ookinetes, many of which are found either within these cells or immediately adjacent to them. Closer inspection of the SRPN10 overexpressing, parasite-associated cells shows that SRPN10 is at least as abundant in their cytoplasm as in their nuclei (Fig. 1C, insets).
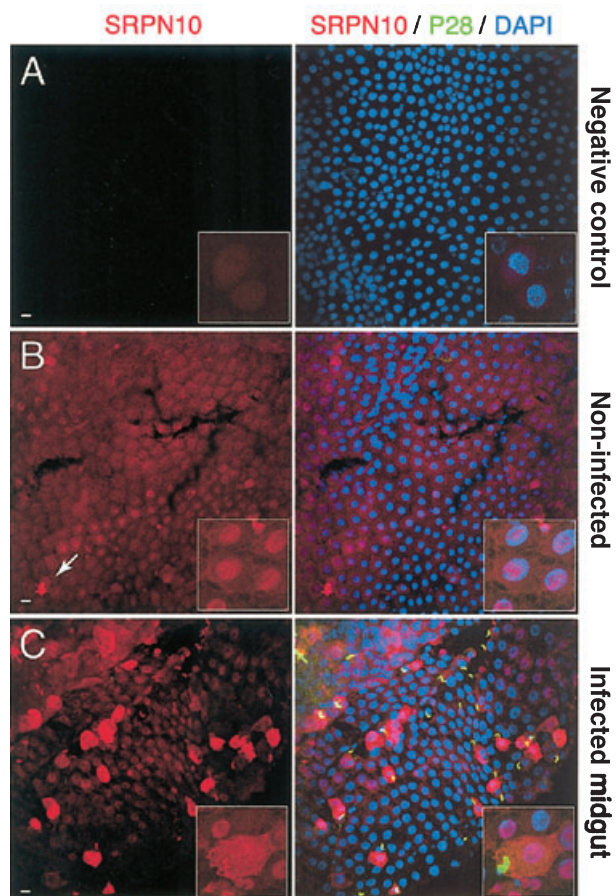

Fig. 1. Low power microscopy views of triple stained, infected and non-infected *A. gambiae* midguts. In the left panels SRPN10 staining in the red channel is shown. Each of the right panels is imaged using three merged channels: SRPN10 is stained in red, parasites are decorated in green using a P28 monoclonal antibody and nuclei are counterstained in blue with DAPI. In each panel representative magnified cells are shown as insets.
A. Mosquito midgut, 25 h PBI (post ingestion of an infected blood meal), stained with SRPN10 preimmune serum and secondary control Alexa488-anti-mouse IgG.
B. Control midgut 25 h after a non-infective blood meal.
C. Mosquito midgut 25 h PBI, showing SRPN10-overexpressing cells in the immediate vicinity of *Plasmodium* ookinetes. All the midguts were treated in the same way in parallel experiments and the image acquisition parameters of the Zeiss LSM 510 confocal microscope were maintained the same for all specimens. Scale bar, 10 μm.

Invaded midgut cells undergo nucleocytoplasmic SRPN10 redistribution, followed by overexpression

According to the 'time bomb' model of midgut invasion in *A. stephensi* (Han *et al.*, 2000), wild-type (wt) *P. berghei* ookinetes can cross the midgut by an intracellular route, eliciting a distinctive syndrome of epithelial cell responses. This includes release of immunostainable parasite-derived P28 surface protein into the invaded cytoplasm; changes in cell shape associated with actin redistribution; a related apical protrusion of the invaded cell and its eventual extrusion into the midgut lumen; and apoptotic

cell death (Han *et al*., 2000; Zieler and Dvorak, 2000; Vlachou *et al*., 2004). We used immunofluorescence and confocal microscopy analysis to examine how the SRPN10 expression pattern might relate to these cellular changes and potentially suggest a link (positive or negative) between SRPN10 products and apoptosis. Our SRPN10 antibody detects serpins equally well in *A. gambiae* and *A. stephensi*, permitting comparative analysis of midgut invasion in both species. For this analysis we have imaged individual horizontal control sections in the plane of the epithelium (as in Fig. 2A–B and F–G) as well as projections of merged stacks of such sections (Fig. 2C, E, H, J).

The majority of the ookinetes were found in the process of crossing the midgut epithelium and many were unambiguously intracellular according to serial confocal images; every single one of the ookinetes (e.g. Fig. 2C) was associated with an epithelial cell displaying a SRPN10 overexpression or redistribution phenotype. A similar tight correlation between cell invasion and SRPN10 overexpression/redistribution held for epithelial cells where an ookinete was no longer present, but had left incontrovertible evidence of its passage. This evidence included an aggregate of shed P28 parasite protein at the epithelial cell periphery, which we interpret as a parasite entry site (Fig. 2A, ▷), or a nearby intracellular trail of P28 spots (Fig. 2B, dotted ▷). As detailed below, additional evidence included two key morphological markers of epithelial invasion: apical protrusion and dramatic reorganization of the actin cytoskeleton.

In both *A. gambiae* and *A. stephensi*, at 23–30 h PIB (post ingestion of the infected blood meal), ookinete-invaded cells were seen by differential interference contrast microscopy (DIC) to protrude apically into the midgut lumen (Fig. 2D and I respectively). In the horizontal projections of Fig. 2E and J an extracellular ookinete is closely associated with the protruding cell, and is visualized in blue by antibodies corresponding to the parasite proteins P70 or P28. Red-stained SRPN10 is prominent in the cytoplasm of the invaded cell but is primarily localized in the nuclei of its immediate neighbours. Actin reorganization has led to a dense green-stained actin ring (▷) in the invaded cell cytoplasm, a marker suggesting that an actin-based mechanism may be involved in the expulsion of invaded cells (Han *et al*., 2000), in both vectors. The SRPN10-enriched cytoplasm and frequently SRPN10-depleted nuclei of invaded cells are prominent in sections at the most apical (luminal) plane, which barely graze (Fig. 2A) or miss altogether (Fig. 2F) the cytoplasm of non-invaded cells. At this level, apico-lateral parasite entry sites marked by a deposit of the P28 parasite protein are detected at the cell periphery, often associated with an intensely stained cytoplasmic patch of SRPN10 (Fig. 2A). Cytoplasmic accumulation of SRPN10 and the

series of P28 specks that we interpret as marking the trail of the parasite's intracellular passage, can be observed also at deeper planes (Fig. 2B and C). Unlike P28, the internal parasite protein P70, which is subpellicular and associated with the inner parasite vacuole membrane (E. Khater and R.E. Sinden, pers. comm.), as well as GFP (Vlachou *et al*., 2004), leave no imprint of peripheral entry sites or intracellular trails in invaded cells (Fig. 2E and data not shown), indirectly confirming the reality of P28 specks. Chains or clusters of apically protruding invaded cells (Fig. 2F), are seen often in *A. stephensi*, as reported (Han *et al*., 2000), whereas in *A. gambiae* such clusters encompass fewer cells and are mostly doublets (Fig. 2A). We interpret the two invaded cells in Fig. 2A–C as representing a case where a single ookinete entered the cell on the left (at the entry site seen at Fig. 2A, ▷) and then moved within the cytoplasm of the same cell, leaving a trail (Fig. 2B, dotted ▷), before turning and entering the cell on the right with which it is now associated (Fig. 2C).

SRPN10 translocates into the cytoplasm of invaded cells and is overexpressed, irrespective of whether the midgut infection is heavy or entails only a few ookinetes. For example, Fig. 3D depicts a strongly SRPN10-overexpressing cell bearing a P28-marked invasion site (▷), in a midgut that was seen at lower magnification (not shown) to be very lightly infected, with only four ookinetes. Thus, the invasion syndrome that we have described thus far reflects local changes within the invaded cell(s) and is not propagated. However, we have also noted downregulation of SRPN10 staining (Fig. 3E) in cells immediately surrounding the invaded cell(s), suggesting some type of transcellular signalling, which merits closer analysis in the future.

We observed that in doublets of invaded cells, the one with which the ookinete is currently associated shows less SRPN10 staining than the other, apparently first-invaded cell (Figs 2C and 3A). This observation prompted us to perform systematic experiments in which we recorded the dynamic SRPN10 patterns at ordered time intervals PIB both in *A. gambiae* and *A. stephensi*. Figure 3 exemplifies the dynamics in *A. gambiae*. In midguts dissected 20–23 h PIB (Fig. 3C), ookinetes are starting to invade epithelial cells, which do not yet protrude apically into the gut lumen. Concomitantly, SRPN10 translocates from the nucleus to the cytoplasm and concentrates towards the cell periphery, especially near the ookinete entry site (Fig. 3C, ▷; see also Fig. 2A and Fig. 3B). Slightly later, at 22–30 h PIB (Fig. 3D), invaded midgut cells show massive increase in SRPN10 cytoplasmic staining as well as nuclear compaction and condensation. Later still, at 25–30 h PIB (Fig. 3E), the massively SRPN10 expressing invaded cells lose histone staining; the apparent loss of nuclear organization and histones suggests cell death,
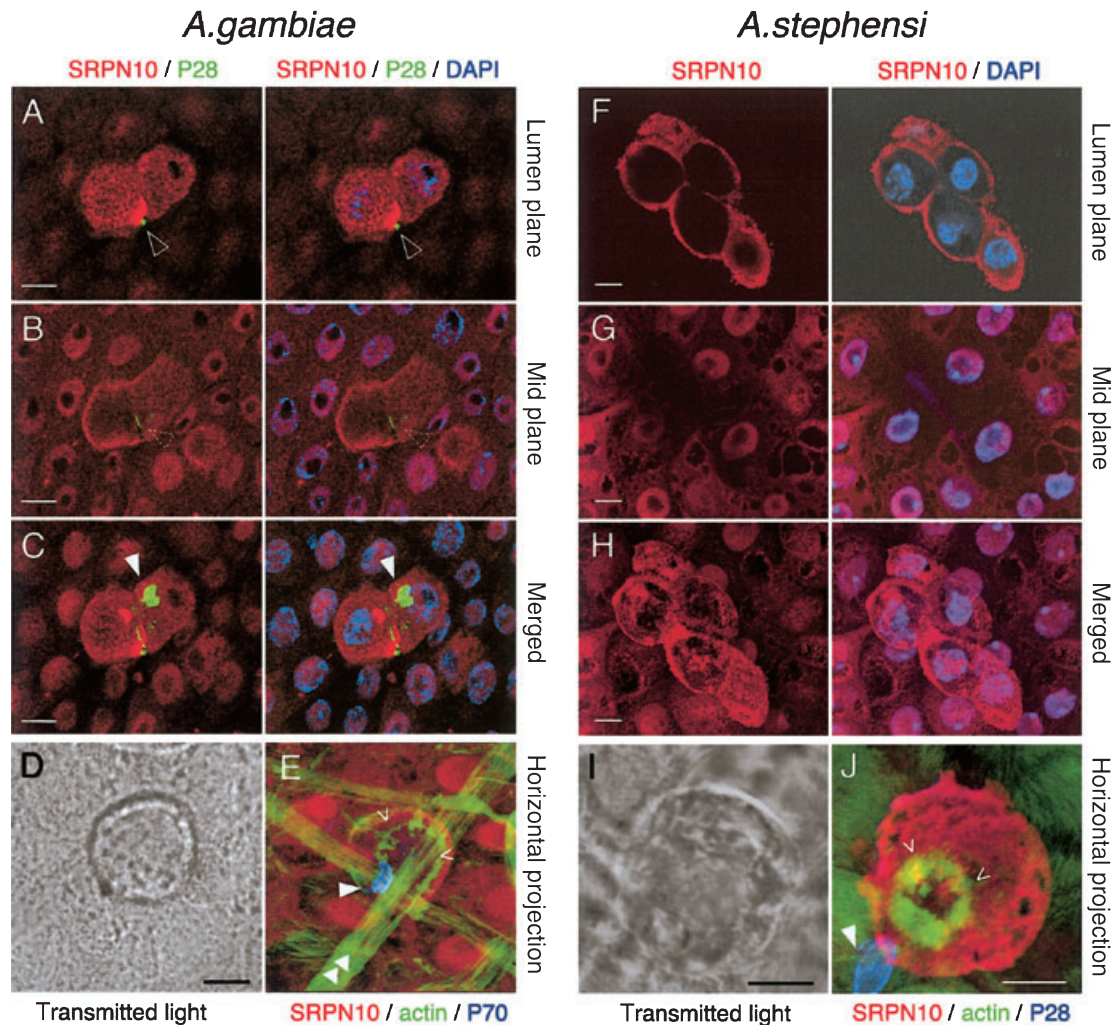
Fig. 2. SRPN10 relocalization and overexpression in *A. gambiae* and *A. stephensi* midgut epithelia invaded by *P. berghei* ookinetes. Scale bars, 10 µm.

A–C. Invasion of *A. gambiae* midgut at 23 h PBI (post ingestion of an infected blood meal); SRPN10 in red; P28 in green; DAPI staining in blue.
A. Single confocal section at the uppermost luminal plane showing protrusion of two invaded cells into the midgut lumen. Note the aggregation of overexpressed SRPN10 around a P28-stained putative entry site (▷). B. Single confocal section at the level of the underlying midgut epithelium revealing the sustained nuclear SRPN10 staining in the non-invaded cells contrasting with a strong peripheral cytoplasmic concentration in the left invaded cell. A trail of intracellular P28 deposits is observed near the boundary between the two invaded cells, most likely marking the site of passage of the ookinete from the left cell to the right. C. Merge of confocal planes generating a horizontal projection view of the epithelium. Note that the ookinete is within the right invaded cell.
D. Interference contrast microscopy (DIC) of an *A. gambiae* invasion region showing apical protrusion of a single invaded cell into the lumen of the gut.
E. Horizontal projection of confocal sections of the same region, with SRPN10 staining in red, phalloidin in green and the ookinete in blue. Note a loose basal actin constriction ring in the invaded cell (>), and the muscles underlying the midgut epithelium (double arrowhead).
F–H. Invaded midgut cell in *A. stephensi*; SRPN10 in red; DAPI staining in blue. F. Confocal section of the uppermost luminal plane showing apical protrusion of a group of five invaded cells into the midgut lumen. In *A. stephensi*, the tendency of *P. berghei* to invade sequentially is pronounced, thereby clusters of invaded cells that are ultimately expelled from the epithelium as a group. In all cells of this group SRPN10 translocates into the cytoplasm, and towards the cell periphery. G. Confocal section at the level of the underlying epithelium showing that healthy cells still exhibit nuclear SRPN10 staining. H. Merged sections generating a horizontal projection.
I. DIC image of an *A. stephensi* invasion region. The invaded cell is protruding into the midgut lumen and the underlying epithelium is out of focus.
J. Horizontal projection of the same invasion region: strong SRPN10 staining in red, phalloidin in green and the ookinete exiting the cell in blue. A thick actin constriction ring is evident (>).

which in other reports has been shown to be apoptotic (Han *et al.*, 2000; Zieler and Dvorak, 2000; Vlachou *et al.*, 2004).

In *A. stephensi* midguts, larger clusters of sequentially

invaded cells have been observed. This allowed us to follow more precisely the temporal dynamics in groups of cells invaded by a single parasite. *A. stephensi* midguts were dissected 24 h and 36 h PIB and invasion events
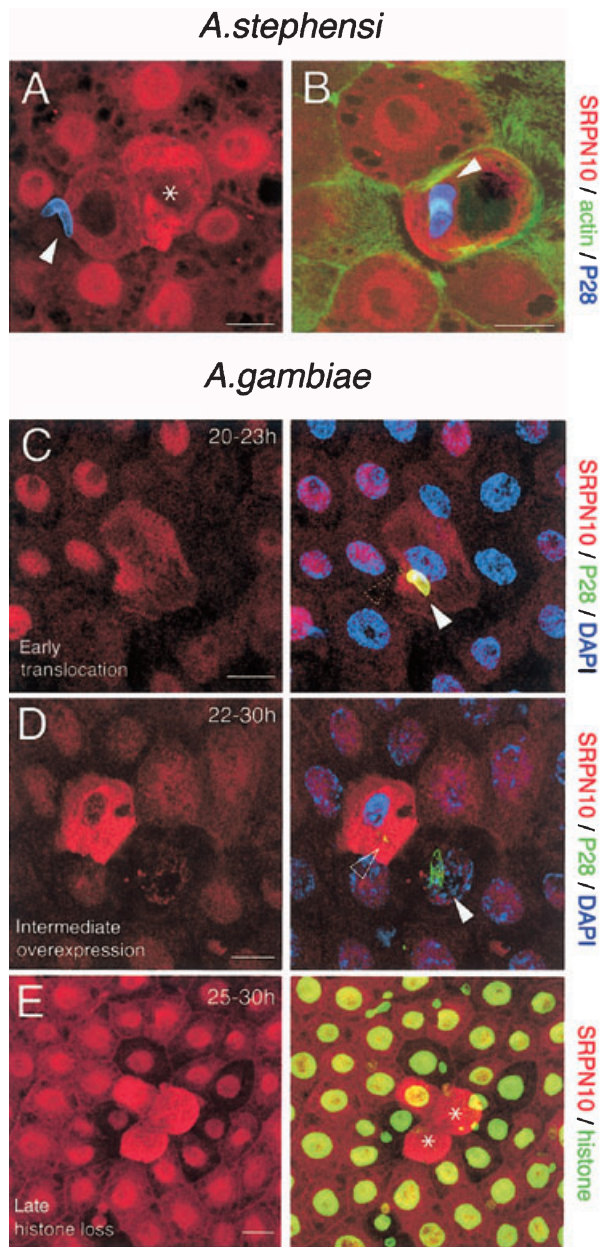
A.stephensi

A.gambiae

Fig. 3. Monitoring epithelial responses through SRPN10 redistribution during the ookinete midgut invasion. All images are horizontal projections.
A. Distinct SRPN10 'phenotypes' are observed in two adjacent *A. stephensi* midgut cells that are surrounded by un-invaded cells showing the typical nuclear concentration of SRPN10 (red). The P28-stained parasite is in blue. The cell more distal to the parasite (*) shows SRPN10 overexpression, while the other close to the parasite exhibits only serpin translocation and not yet overexpression.
B. An ookinete appears to be escaping from an invaded cell in *A. stephensi*. SRPN10 in red; phalloidin in green; P28 in blue. The serpin has translocated from the nucleus to the cytoplasm.
C–E. A timed sequence of ookinete invasions marked by SRPN10 in *A. gambiae*. Images on the left are stained in red for SRPN10 only, those on the right are also stained for the parasite P28 surface protein in green and nuclei in blue (C and D) or histones in green (E). C. Early invasion phase marked by SRPN10 translocation to the cytoplasm, especially the periphery. The ookinete has penetrated the cell in the middle, leaving a trail of P28 specks that identify the invasion site (dotted ▷). D. Intermediate invasion phase/overexpression. The parasite has escaped from the invaded cell, which is marked by heavy serpin concentration in the cytoplasm, and nuclear shrinkage; chromatin condensation starts to be evident. Note the parasite entry site (▷). E. Late phase. The loss of nuclear organization in invaded cells is evident by the lack of histone staining (*). Note also the decrease of SRPN10 levels in un-invaded neighbouring cells. Scale bars, 10 μm.

plasmic staining at relatively low expression levels; and O, overexpression of SRPN10 to high levels.
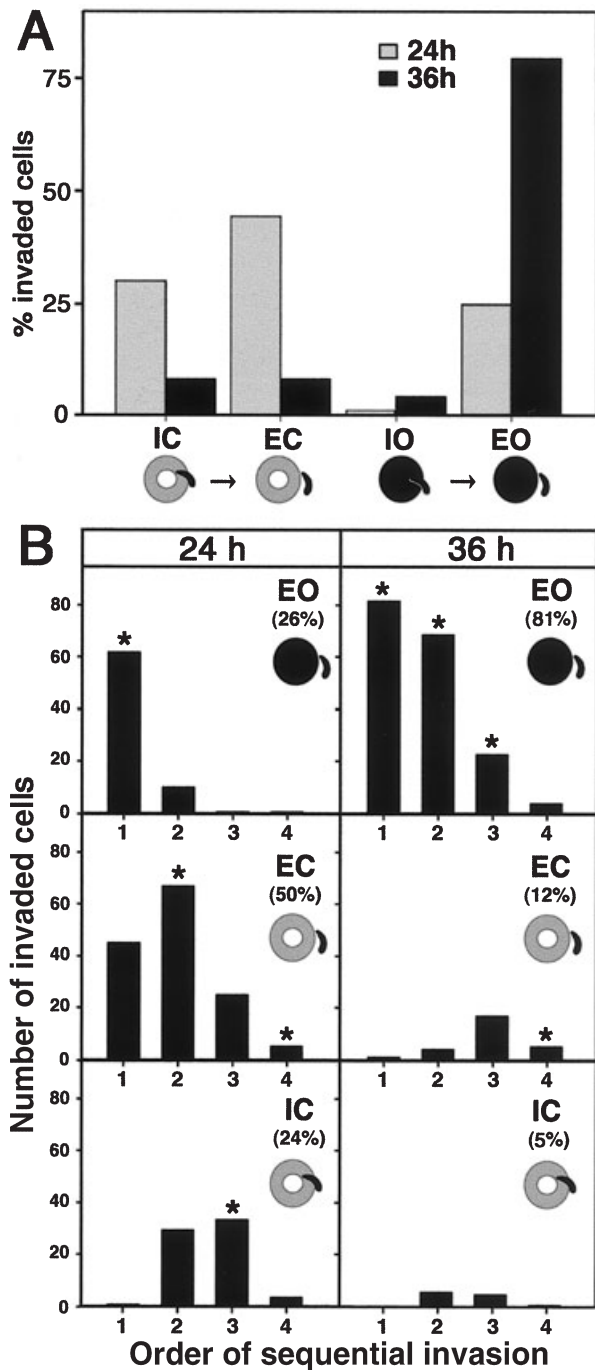
Single and multiple cell invasions were analysed separately. At 24 h and 36 h 48% and 46% were single-cell invasions, respectively, and the rest multiple-cell lateral invasions (two to four cells). In the case of single-cell invasions many of the cells overexpressing SRPN10 had undergone extensive degeneration, so that the nuclear compartment was not well-defined or was even absent in some cases (see also Fig. 3E). The C phenotype was predominated at 24 h but relatively rare at 36 h (74% and 16% of the events respectively. Conversely, the O (overexpression) phenotype increased in frequency, from 26% at 24 h to 84% at 36 h (Fig. 4A). Similarly, the O phenotype increased over time in sequential invasions, from 26% at 24 h to 84% at 36 h (Fig. 4B). Thus, cells with relatively low levels of cytoplasmic SRPN10 at 24 h, are likely to overexpress the protein by 36 h PIB.

Intracellular ookinetes were 31% of the total at 24 h PIB (I, observed in the middle plane with at least a portion inside the invaded cell), but became more rare (12%) at 36 h (Fig. 4A). Cells overexpressing SRPN10 while the ookinete was intracellular were rare (1% and 4% of single-cell invasions at 24 and 36 h PIB respectively). In most cases parasites were extracellular (E, in the basal epithelial plane, already outside the cell) when cells overexpressed serpin (Fig. 4A). These data confirm that serpin overexpression is a relatively late event, usually taking place after parasite invasion has been completed.

Sequential, multiple-cell lateral invasions proved very useful to infer the successive appearance of distinct SRPN10 phenotypes. By definition, in these events more

were recorded. All events included in the analysis represent intracellular invasions as it was possible to see accumulation of P28 at the invasion site and P28 trails when multiple cells were invaded laterally by the same parasite.

At 24 and 36 h PIB, 204 and 152 invading ookinetes were analysed, which crossed 379 and 289 midgut epithelial cells respectively. Epithelial cells from females fed on an un-infected mouse were also analysed (856 cells at 24 h and 873 at 36 h PIB). SRPN10 was localized predominantly in the nucleus in 99.2% (24 h) and 99.4% (36 h) of healthy un-invaded cells, whereas it translocated to the cytoplasm in all 668 invaded cells. Two distinct SRPN10 expression phenotypes predominated: C, cyto-

A

B

Fig. 4. Quantitative dynamics of SRPN10 redistribution and overexpression in *A. stephensi* midgut epithelial cells at 24 h and 36 h post infection.
A. Percentage of single-cell invasions showing cytoplasmic redistribution (C) or strong overexpression (O) of SRPN10, in cells where the parasite is still intracellular (I) or has exited basally (E). The four possible phenotypes (IC, EC, IO, EO) are identified with corresponding icons. Note the shift from predominant redistribution at 24 h to predominant overexpression at 36 h.
B. Numbers of cells in sequential invasion events, phenotyped (with accompanying icons) as in Panel A and plotted in the order of invasion (first to fourth invaded cells). Only three cells with an IO phenotype were observed in this study and their distribution does not appear in the graph. Note that, by definition, the elapsed post-invasion time is highest for first invaded cells, followed by the times for second, third, and fourth invaded cells; therefore, the 24 h data show that the IC phenotype is earliest (maximal in third invaded cells), EC is next (maximal in second invaded cells) and EO is the latest (maximal in first invaded cells). The 36 h data indicate the same sequence of phenotypes, but shifted towards the latest phenotype (EO). Asterisks indicate the most frequent phenotypes in each case.

fourth invaded cells. The progression was similar at 36 h (albeit at an overall higher expression level); overexpression was observed in 99%, 88%, 51% and 40% of the first, second, third and fourth invaded cells respectively. It should be noted that in sequential invasions, cells overexpressing SRPN10 while the parasite was still completely intracellular were again rare: none were detected at 24 h and only three (1% of the events) at 36 h.

Mutant parasites lacking P25 and P28 surface proteins are deficient in induction of SRPN10 redistribution/overexpression

The related, GPI-anchored P25 and P28 proteins are major components of the ookinete plasma membrane in all *Plasmodium* species. Antibodies against these proteins interfere with ookinete development and oocyst formation and are potential transmission-blocking agents (Kaslow, 1997). The proteins are apparently functionally additive, as single knockout transgenic parasites (sKO) exhibit very mild phenotypes compared with the double knockouts (P25/28 dKO) (Tomas *et al.*, 2001). The latter are sensitive to the hostile midgut environment and severely compromised in ookinete and oocyst development; however, small numbers of dKO ookinetes do cross the epithelium and form oocysts. Considering the deposition of P28 at parasite entry sites and its intracellular shedding in midgut cells, we tested whether P25/28 dKO ookinetes elicit the various midgut epithelial reactions, including dynamic SRPN10 expression and localization patterns. For this purpose we compared midguts of mosquitoes that were matched in age and fed in parallel on mice infected with either wt or dKO parasites. The midguts were dissected and fixed at 24–31 h PIB, and were stained with antibodies to SRPN10 and either P28 (for wt) or P70 (for dKO parasites). We scored hundreds of invad-

time had elapsed from the invasion of the first cell (identifiable by the staining of the invasion site) than of the second, more from the invasion of the second than of the third cell, etc. Therefore, assuming a progression from cytoplasmic relocalization to overexpression of SRPN10, we would expect the proportion of overexpression to be highest for first invaded cells and to decline gradually for the second, third and fourth cells. Indeed, at 24 h overexpression was observed in 58% of the first invaded cells but only very few of the second (9%) and none of third or

ing ookinetes by whether or not they were closely associated with cells showing SRPN10 translocation and overexpression; we excluded ookinetes in the process of lysis (which is common in the dKO strain), ookinetes merely attached to the epithelial surface before invasion, or those that were rounding up to form oocysts. All scored ookinetes had a DAPI-stained nucleus and a reasonably preserved shape. At 24 h PIB, hundreds of wt ookinetes crossing the midgut met these criteria and were scored (495 in *A. gambiae* and 1048 in *A. stephensi*). The dKO ookinetes that met these criteria were *c.* 20-fold less numerous (28 and 46 respectively; Fig. 5A).

Wild-type parasites in the process of cell egress as well as parasites outside but closely associated with a SRPN10-overexpressing cell (presumably ookinetes recently emerged into the subepithelial space) accounted for 89% of the total in *A. gambiae* and 85% in *A. stephensi*. The rest were probably emerged ookinetes that had moved within the subepithelial space, away from the previously invaded cells (Han *et al.*, 2000). However, we cannot exclude the formal possibility that some ookinetes may have crossed the epithelium by an alternative, intercellular route that does not induce SRPN10 overexpression.

In contrast, of the dKO ookinetes that could be scored, only 11% were associated with a SRPN10 overexpressing cell, in either species (Fig. 4A). Indeed, only three cases were scored as intracellular ookinetes (in *A. stephensi*). Comparable differences between wt and dKO parasites, in terms of the numbers that could be scored and the numbers associated with SRPN10 overexpressing cells, were also detected at a later time point (31 h PIB; data not shown). An additional clear difference was that in the case of wt but not dKO ookinetes, invasion was associated with epithelial cell protrusion. For example, the horizontal projection of an invaded epithelium in Fig. 5C shows a cell intensely strained with SRPN10, adjacent to a wt ookinete that has emerged; the pseudocross-section of Fig. 5B shows the same cell bulging apically into the lumen. In contrast, Fig. 5F shows the horizontal projection of an epithelium infected with dKO parasites (many of which
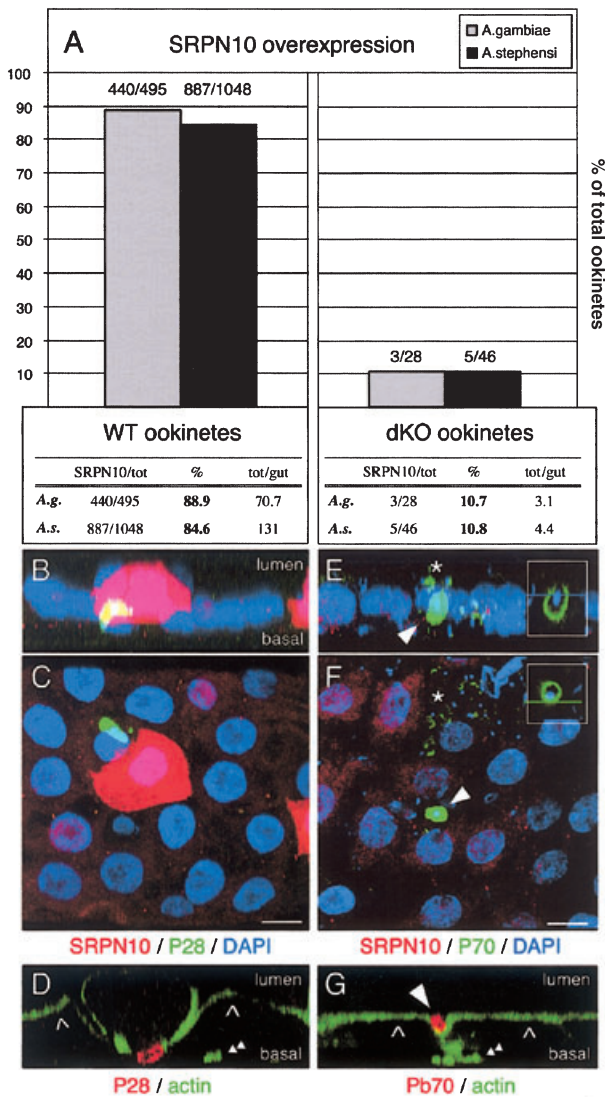

Fig. 5. *Plasmodium berghei* ookinetes lacking P28, P25 proteins fail to elicit SRPN10 translocation/overexpression in the midguts of *A. stephensi* and *A. gambiae*.
A. Numbers and percentages of invading ookinetes that elicit SRPN10 relocalization and/or overexpression 24 h PIB (post ingestion of the infected blood meal) in *A. gambiae* (grey bars) and *A. stephensi* (black bars).
B and C. Projections of a representative wt ookinete invasion region in *A. gambiae*; SRPN10 in red; ookinete in green; DAPI in blue. Scale bar, 10 μm. B. Pseudocross-section (lateral projection) of epithelium invaded by a wt ookinete. The invaded cell shows massive accumulation of SRPN10 in the cytoplasm and protrudes apically into the gut lumen. The parasite is emerging at the basal side. C. Horizontal projection of the same invasion region.
D. Single lateral cross-section, stained with phalloidin (green) and Pb28 (red), 23 h PIB in *A. gambiae*. Note the absence of actin-filled apical microvilli and the reorganization of actin in the invaded cell, which protrudes into the gut lumen. Vertical arrows (∧) point the microvillar layer in flanking cells. The ookinete is exiting at the basal side, which is defined by the presence of muscles (double arrowhead).
E and F. Projections of a representative dKO ookinete invasion region in *A. gambiae*; SRPN10 in red; ookinete in green; DAPI in blue. Scale bar, 10 μm. E. Pseudocross-section (lateral projection) of invaded epithelium. An ookinete is crossing the epithelial layer. Note the absence of SRPN10 overexpression and cell protrusion, as indicated by the uniform location of the nuclei in the same plane (blue). Lysed parasites can be detected at the luminal side of the midgut (*). F. Horizontal projection of the same dKO invasion region, clearly showing the lack of SRPN10 overexpression. Dispersed green and blue material corresponds to parasite cytoplasmic and nuclear debris. Insets in E and F magnify details of the healthy dKO invading ookinete showing the presence of an intact nucleus, and a well-defined layer of P70 material. G. Absence of cell protrusion in a dKO invasion region. The ookinete is wedged between two epithelial cells in the intercellular space outlined by actin. The orientation of the epithelium is defined by a group of midgut muscles (double arrowhead). Vertical arrows (∧) show the regular microvillar layer retained by two epithelial cells flanking the invading dKO parasite.

have lysed); a single healthy ookinete is seen surrounded by epithelial cells, none of which display SRPN10 upregulation. The corresponding pseudocross-section (Fig. 5E) shows that this ookinete has penetrated deeply into the epithelium, but has not elicited cell protrusion or SRPN10 induction.

Pseudocross-sections stained for actin with phalloidin display favourably the actin cytoskeleton and its reorganization after invasion by wt but not dKO parasites. Figure 5D presents a cell invaded by a wt ookinete (which is emerging basally). This invaded cell is clearly protruding into the gut lumen, and is missing the regular apical microvillar layer, unlike the flanking non-invaded cells (Fig. 5D, ∧). The actin of the invaded cell has been redistributed laterally, and also forms a basal actin ring just above the exiting parasite. In contrast, Fig. 5G shows preservation of the epithelial structure during invasion by a dKO ookinete: the parasite is wedged between two epithelial cells both of which retain their regular microvillar layer (Fig. 5G, ∧). The lateral interface of these cells is outlined by actin, and the ookinete appears to be taking an intercellular route. However, the evidence at hand is insufficient to establish unequivocally whether dKO ookinetes invade by an intercellular route, in contrast to the major (and possibly exclusive) intracellular route that is followed by wt parasites.

Discussion

We have demonstrated that progressive intracellular redistribution and subsequent massive upregulation of SRPN10 are robust, cell-autonomous markers of the major, intracellular route of *P. berghei* ookinete invasion, in both *A. stephensi* and *A. gambiae*. We have detected numerous wt ookinetes closely associated with midgut cells exhibiting SRPN10 redistribution and/or overexpression at broad time intervals (20–36 h) following an infected blood meal. The functional significance of SRPN10 overexpression/redistribution remains to be established, as well as the identity of the respective target proteases.

Recently, several members of the serpin family have been found localized to various extent in the cell nucleus: passive diffusion through nuclear pores (Bird *et al.*, 2001), specific nuclear export/import signals (Rodriguez *et al.*, 2003), as well as interactions with either chromatin or target proteases (Irving *et al.*, 2000) have been suggested as mediators of this subcellular topology. The presence of a serpin in the nucleus may be related to the inactivation of proteases, either normally present or introduced therein following induction of apoptosis. For example, the serpin MENT (Myeloid and Erythroid Nuclear Termination stage-specific protein) accumulates in the nucleus of terminally differentiated avian blood cells, promoting a block in proliferation and strong condensation of the chromatin,

possibly through the regulation of a nuclear cysteine proteinase (Irving *et al.*, 2002). This may be considered a case of arrested apoptosis in the nucleus, while nucleocytoplasmic shuttling of cowpox virus-encoded antiapoptotic serpin CrmA (a specific inhibitor of caspase 1, caspase 8 and granzyme B), has been suggested as an efficient mechanism to inhibit cellular pro-apoptotic proteases in both cellular compartments (Rodriguez *et al.*, 2003). An increase in active, parasite-derived proteases, first in the cell periphery and then deeper in the cytoplasm of invaded midgut cells, may be hypothesized as the apoptotic trigger accompanying invasion, and may also serve as the driving force for the observed induction and dynamically changing subcellular localization of SRPN10 serpins.

Lately we obtained additional evidence indicating that SRPN10 overexpression is under the control of apoptotic signals. In *A. stephensi* transgenes, in which a LacZ marker was indirectly placed under the transcriptional control of a SRPN10 promoter fragment, we observed β-gal staining patterns well correlated with the onset of midgut morphogenesis during the larval to pupal transition. Midgut remodelling at this stage is accompanied by programmed cell death (Lycett *et al.*, 2004).

Some role of SRPN10 related to the induction of apoptosis in wt parasite-invaded midgut epithelial cells, is very likely. Apoptosis at the ookinete invasion sites has been reported previously (Zieler and Dvorak, 2000; Vlachou *et al.*, 2004), and is a centrepiece of the 'time-bomb' theory of invasion (Han *et al.*, 2000). Indeed, we have noted that tissue injury during midgut dissection, even in the absence of parasites, is correlated with sporadic SRPN10 overproduction (Fig. 1B). Extensive mutagenesis and reverse genetic manipulations would be necessary to uncover the molecular mechanisms that drive SRPN10 levels and changes in subcellular localization in normal and parasite-invaded apoptotic cells.

Whatever its inherent function, SRPN10 upregulation is a powerful tool for analysis of midgut invasion processes. It has permitted convenient validation of the 'time bomb' theory, not only in *A. stephensi* where it was initially proposed, but also in *A. gambiae*, thus indicating conserved mechanisms of invasion. It has also pointed out major differences between invasion by wt or dKO ookinetes, which merit further detailed analysis. Surprisingly, a careful recent study has indicated that SRPN10 is not upregulated at the RNA level in the midguts of *A. gambiae* females fed on *P. falciparum* infected volunteers (Tahar *et al.*, 2002). An explanation might be that parasite levels in these natural infections are usually low (Pringle, 1966; Collins *et al.*, 1984), and even the sensitive real time PCR analysis may have failed to reveal the cell-autonomous SRPN10 upregulation at the RNA level, because it is limited to a small number of invaded cells. Alternatively,

P. falciparum may indeed follow an invasion route in *A. gambiae* different than that of *P. berghei*. This important question can be resolved in future studies by using the SRPN10 antibody to follow *P. falciparum* invasion.

Few *Anopheles* genes with altered expression levels during midgut invasion have been reported to date, and among them SRPN10 is the only one characterized in terms of its spatial expression at the cellular and subcellular level. Another gene that is heavily overexpressed in infected midguts is TEP4, which encodes a member of the complement/α2-macroglobulin superfamily (Oduol *et al.*, 2000; Christophides *et al.*, 2002); however, its spatial expression pattern has not been studied. In humans α2-macroglobulin is thought to be the major inhibitor of serum proteases and the important group of matrix metalloproteases (Baker *et al.*, 2002). Although the indications are fragmentary to date, the overexpression of TEP4 and the cell-autonomous overexpression of SRPN10, together with the remarkable shedding of a subtilisin-like ookinete serine protease (SUB2) into the cytosol of *A. stephensi* midgut cells invaded by *P. berghei* (Han *et al.*, 2000), are highly intriguing: they suggest that parasite-induced as well as endogenous proteolytic pathways and their modulators in parasite-invaded cells are worthy of intensive study.

Experimental procedures

Mosquito rearing

A. gambiae strain G3 and *A. stephensi* were reared at 27°C at a relative humidity of 75%, with a 12/12 h light/darkness cycle. Larvae were raised in 0.1% marine salt water and fed with powdered cat food. Adults were fed *ad libitum* on wet cotton, soaked in 15% sucrose solution. To complete the life cycle, females were allowed to take a blood meal on anaesthetised BALB/c or Swiss Webster mice. *P. berghei* strain 234 and the P25/P28 double knockout (dKO) strain (Tomas *et al.*, 2001) were maintained in BALB/c mice by blood passage. The parasitaemia of infected mice was checked by light microscopy of blood-smears counterstained with Giemsa solution (Sigma). For blood stage passages, 100–200 µl of blood of an infected mouse (parasitaemia 10–20%) was injected into a healthy mouse. A maximum of 10 passages was performed before a fresh aliquot of blood stage parasites was defrozen. To increase parasite loads mice were treated with phenyl hydrazine (6 mg ml^{-1}, 200 µl subcutaneous injection) 3 days before passage; un-infected mice controls were treated the same. Only mice with erythrocyte infection rates above 8% in 3–4 days post injection were used for experiments. Mosquito females were allowed to take a blood meal on infected or control BALB/c mice at 19°C for 45 min, and were kept at 19°C to allow parasite development until dissection.

Immunofluorescence

The generation of the SRPN10 antiserum was previously reported (Danielli *et al.*, 2003). Briefly, a purified His-tag-SRPN10 fusion protein was used to immunize two rabbits. After final bleeding the antiserum was affinity purified using a recombinant GST-SRPN10 fusion protein coupled to CNBr-activated Sepharose 4B (Pharmacia). The resulting affinity-purified antiserum was checked on immunoblots (1:1000) for absence of cross-reactivity before use for immunostaining. Dissected midguts were prefixed for 90 s in fixative (1× PBS, 4% formaldehyde, 2 mM MgSO$_4$, 1 mM EGTA, pH 7.2), transferred to ice-cold PBS and cut open with microdissection scissors. The blood meal was carefully removed and the epithelium fixed for another 45–60 min. Samples were washed twice in PBS for 15 min and blocked in PBT (1% BSA, 0.1% Triton X-100, PBS). Primary antibodies were incubated overnight at 4°C, washed three times for 20 min and incubated 1 h with secondary antibodies, all in PBT. After two washes of 20 min in PBT, nuclei were counterstained with DAPI or To-Pro 3 (1:1000, Molecular Probes) for 5 min. Guts were further washed in PBT for 15 min, flattened and mounted in Pro-Long antifading reagent (Molecular Probes). For the counterstaining of actin, Phalloidin-Alexa488 (Molecular Probes) was added to the washing solution 10 min before mounting the samples (6 µM solution in MeOH, 1:200). All samples were analysed using a Zeiss LSM 510 confocal microscope. Primary antibody dilutions: 1:333 serpin SRPN10; 1:300 Pbs21 mAb 13.1; 1:150 Pb70 mAb; 1:500 histones MAB052 (Chemicon). Secondary antibody dilutions: 1:1000 Cy3-, Cy5-conjugated, goat anti-mouse, anti-rabbit IgGs (Jackson Laboratories); 1:1500 Alexa488-, Alexa546-conjugated goat anti-mouse and anti-rabbit IgGs (Molecular Probes).

References

Adams, M.D., Celniker, S.E., Holt, R.A., Evans, C.A., Gocayne, J.D., Amanatides, P.G., *et al.* (2000) The genome sequence of *Drosophila melanogaster*. *Science* **287:** 2185–2195.

Baker, A.H., Edwards, D.R., and Murphy, G. (2002) Metalloproteinase inhibitors: biological actions and therapeutic opportunities. *J Cell Sci* **115:** 3719–3727.

Bird, P.I. (1998) Serpins and regulation of cell death. *Results Probl Cell Differ* **24:** 63–89.

Bird, C.H., Blink, E.J., Hirst, C.E., Buzza, M.S., Steele, P.M., Sun, J., *et al.* (2001) Nucleocytoplasmic distribution of the ovalbumin serpin PI-9 requires a nonconventional nuclear import pathway and the export factor Crm1. *Mol Cell Biol* **21:** 5396–5407.

Christophides, G.K., Zdobnov, E., Barillas-Mury, C., Birney, E., Blandin, S., Blass, C., *et al.* (2002) Immunity-related genes and gene families in *Anopheles gambiae*. *Science* **298:** 159–165.

Collins, F.H., Zavala, F., Graves, P.M., Cochrane, A.H., Gwadz, R.W., Akoh, J., and Nussenzweig, R.S. (1984) First field trial of an immunoradiometric assay for the detec-

tion of malaria sporozoites in mosquitoes. *Am J Trop Med Hyg* **33:** 538–543.

Collins, F.H., Sakai, R.K., Vernick, K.D., Paskewitz, S., Seeley, D.C., Miller, L.H., *et al.* (1986) Genetic selection of a *Plasmodium*-refractory strain of the malaria vector *Anopheles gambiae. Science* **234:** 607–610.

Danielli, A., Kafatos, F.C., and Loukeris, T.G. (2003) Cloning and characterization of four *Anopheles gambiae* serpin isoforms, differentially induced in the midgut by *Plasmodium berghei* invasion. *J Biol Chem* **278:** 4184–4193.

Han, Y.S., Thompson, J., Kafatos, F.C., and Barillas-Mury, C. (2000) Molecular interactions between *Anopheles stephensi* midgut cells and *Plasmodium berghei*: the time bomb theory of ookinete invasion of mosquitoes. *EMBO J* **19:** 6030–6040.

Holt, R.A., Subramanian, G.M., Halpern, A., Sutton, G.G., Charlab, R., Nusskern, D.R., *et al.* (2002) The genome sequence of the malaria mosquito *Anopheles gambiae. Science* **298:** 129–149.

Irving, J.A., Pike, R.N., Lesk, A.M., and Whisstock, J.C. (2000) Phylogeny of the serpin superfamily: implications of patterns of amino acid conservation for structure and function. *Genome Res* **10:** 1845–1864.

Irving, J.A., Shushanov, S.S., Pike, R.N., Popova, E.Y., Bromme, D., Coetzer, T.H., *et al.* (2002) Inhibitory activity of a heterochromatin-associated serpin (MENT) against papain-like cysteine proteinases affects chromatin structure and blocks cell proliferation. *J Biol Chem* **277:** 13192–13201.

Kanost, M.R. (1999) Serine proteinase inhibitors in arthropod immunity. *Dev Comp Immunol* **23:** 291–301.

Kaslow, D.C. (1997) Transmission-blocking vaccines: uses and current status of development. *Int J Parasitol* **27:** 183–189.

Kruger, O., Ladewig, J., Koster, K., and Ragg, H. (2002) Widespread occurrence of serpin genes with multiple reactive centre-containing exon cassettes in insects and nematodes. *Gene* **293:** 97–105.

Ligoxygakis, P., Pelte, N., Hoffmann, J.A., and Reichhart, J.M. (2002a) Activation of *Drosophila* toll during fungal infection by a blood serine protease. *Science* **297:** 114–116.

Ligoxygakis, P., Pelte, N., Ji, C., Leclerc, V., Duvic, B., Belvin, M., *et al.* (2002b) A serpin mutant links Toll activation to melanization in the host defence of *Drosophila. EMBO J* **21:** 6330–6337.

Ligoxygakis, P., Roth, S., and Reichhart, J.M. (2003) A serpin regulates dorsal-ventral axis formation in the *Drosophila* embryo. *Curr Biol* **13:** 2097–2102.

Lycett, G., Kafatos, F.C., and Loukeris, T.G. (2004) Conditional expression in the malaria mosquito *A. Stephensi* with Tet-On and Tet-Off systems. *Genetics* (in press).

Oduol, F., Xu, J., Niare, O., Natarajan, R., and Vernick, K.D. (2000) Genes identified by an expression screen of the vector mosquito *Anopheles gambiae* display differential molecular immune response to malaria parasites and bacteria. *Proc Natl Acad Sci USA* **97:** 11397–11402.

Pringle, G. (1966) A quantitative study of naturally-acquired malaria infections in *Anopheles gambiae* and *Anopheles funestus* in a highly malarious area of East Africa. *Trans R Soc Trop Med Hyg* **60:** 626–632.

Rodriguez, J.A., Span, S.W., Kruyt, F.A., and Giaccone, G. (2003) Subcellular localization of CrmA: identification of a novel leucine-rich nuclear export signal conserved in anti-apoptotic serpins. *Biochem J* **373:** 251–259.

Silverman, G.A., Bird, P.I., Carrell, R.W., Church, F.C., Coughlin, P.B., Gettins, P.G., *et al.* (2001) The serpins are an expanding superfamily of structurally similar but functionally diverse proteins. Evolution, mechanism of inhibition, novel functions, and a revised nomenclature. *J Biol Chem* **276:** 33293–33296.

Sinden, R.E. (1999) Plasmodium differentiation in the mosquito. *Parassitologia* **41:** 139–148.

Tahar, R., Boudin, C., Thiery, I., and Bourgouin, C. (2002) Immune response of *Anopheles gambiae* to the early sporogonic stages of the human malaria parasite *Plasmodium falciparum. EMBO J* **21:** 6673–6680.

Tomas, A.M., Margos, G., Dimopoulos, G., van Lin, L.H., de Koning-Ward, T.F., Sinha, R., *et al.* (2001) P25 and P28 proteins of the malaria ookinete surface have multiple and partially redundant functions. *EMBO J* **20:** 3975–3983.

Vernick, K.D., Fujioka, H., Seeley, D.C., Tandler, B., Aikawa, M., and Miller, L.H. (1995) Plasmodium gallinaceum*: a refractory mechanism of ookinete killing in the mosquito,* Anopheles gambiae. *Exp Parasitol* **80:** 583–595.

Vlachou, D.T.Z., Zimmerman, T., Cantera, R., Janse, C.J., Waters, A.P., and Kafatos, F.C. (2004) Real-time, *in vivo* analysis of malaria ookinete locomotion and mosquito midgut invasion. *Cell Microbiol* **6:** 671–685.

Zieler, H., and Dvorak, J.A. (2000) Invasion *in vitro* of mosquito midgut cells by the malaria parasite proceeds by a conserved mechanism and results in death of the invaded midgut cells. *Proc Natl Acad Sci USA* **97:** 11516–11521.